Journal of Physics: Conference Series **500** (2014) 052018 doi:10.1088/1742-6596/500/5/052018

Modelling an IHE experiment with a suite of DSD models

A N Hodgson

AWE, Aldermaston, Reading, Berkshire, RG7 4PR, UK

E-mail: alex.hodgson@awe.co.uk

Abstract. At the 2011 APS conference, Terrones, Burkett and Morris published an experiment primarily designed to allow examination of the propagation of a detonation front in a 3-dimensional charge of PBX9502 insensitive high explosive (IHE). The charge is confined by a cylindrical steel shell, has an elliptical tin liner, and is line-initiated along its length. The detonation wave must propagate around the inner hollow region and converge on the opposite side. The Detonation Shock Dynamics (DSD) model allows for the calculation of detonation propagation in a region of explosive using a selection of material input parameters, amongst which is the $D(K)$ relation that governs how the local detonation velocity varies as a function of wave curvature. In this paper, experimental data are compared to calculations using the 2D DSD and newly-developed 3D DSD codes at AWE with a variety of $D(K)$ relations.

1. Introduction

The 'IHE experiment' was designed and fired at Los Alamos National Laboratory (LANL) to measure detonation propagation around an elliptical hole within a circular cylinder of PBX9502 [1]. As shown in figures 1 and 2, the cylinder is confined by an outer steel liner and inner tin liner, and has a depth of 10 cm. The charge is initiated along the entire cylinder depth by a PBX9501 booster which is itself initiated with a line-wave generator. This initiation train is inclined at a 30° angle to the major axis of the inner ellipse. Detonation wave propagation is captured by a series of proton radiography density maps.

Prediction of detonation wave propagation in high explosive can be achieved using a number of methods. The Detonation Shock Dynamics (DSD) model allows for the variation in local detonation velocity, D, with wave curvature, K. As the overall detonation wave curvature increases the propagation speed reduces. This effect is greater for less-ideal explosives such as IHE due to the steepness of the $D(K)$ relation. For the IHE experiment, the asymmetric cylindrical charge of PBX9502 means that the speed of detonation propagation will differ between the upper and lower regions, so the data can be used in DSD model validation. In DSD the angle the detonation wave makes with a charge boundary is constrained to a maximum value dependent on the adjacent material.

Predictions of detonation propagation in the IHE experiment were made by Terrones et al [1]. The 3D hydrocode PAGOSA was used in conjunction with programmed burn, DSD and Forest Fire models. From these it was concluded that DSD gives the best overall reproduction of data under fine mesh resolution. In this work we aim to quantify burn-time differences in DSD from firstly applying various existing $D(K)$ relations for PBX9502, and secondly by comparing

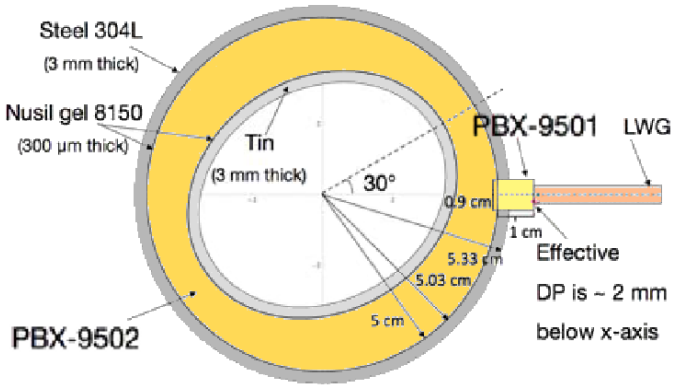

Figure 1. Cross-section schematic of the IHE experiment, from [1]. The booster is initiated with a line wave generator (LWG), giving rise to an effective detonation point (DP) in the DSD calculation.

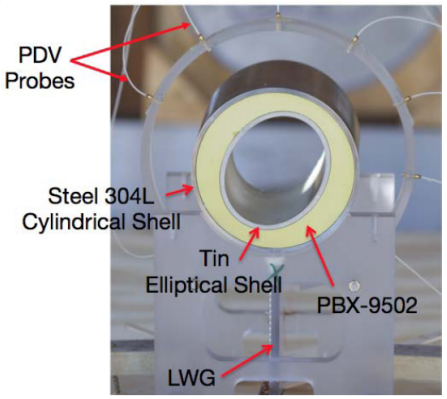

Figure 2. Assembly view of the experiment, from [1].

results using AWE's DSD codes in 2D and 3D. Both codes use a level-set scheme to propagate the detonation wave through a conformal mesh, having the advantage over an Eulerian mesh in that the HE-inert boundaries are explicitly defined. The conformal mesh is generated in 2D by an in-house Lagrangian hydrocode and in 3D by the PMESH meshing code developed at Lawrence Livermore National Laboratory.

2. Validation procedure

2.1. DSD methodology

To model the DSD detonation wave propagation in PBX9501 and PBX9502 explosives, a number of $D(K)$ relations are selected from independent analyses of rate-stick wave-shape data. A single relation for PBX9501 is used based on analysis by T Aslam et al [2]. Three $D(K)$ relations for PBX9502 are used, from publications by Aslam [3] and L Hill et al [4], and a relation produced by D Swift [5] using a set of rate-stick data from LANL. The Aslam and Swift relations were each calibrated to 7 wave-shapes from rate-sticks machined from recycled material. The Hill relation used the same data with 15 additional wave-shapes at different starting temperatures, material lots and initial densities. The relations are shown in figure 3, lying reasonably closely despite the different PBX9502 material and the variation in calibration method used in each analysis. In this work we apply DSD analysis to an experiment at ambient temperature with PBX9502 originating from a lot of virgin material. No initial charge densities were quoted in [1], [3] or [5]. The initial density for PBX9502 of $1.890\,\mathrm{g/cm^3}$ is chosen as a baseline value with an uncertainty margin of $\pm 0.005\,\mathrm{g/cm^3}$. Sensitivity to initial density will be investigated within this range, for which three $D(K)$ relations encompassing the full density range are shown in figure 3.

In each rate-stick calibration study, a constraint was applied to the angle of the shock at the charge boundaries. This was performed to produce the best fit to the overall shock shape. The boundary angle may vary by a large amount ($\pm 10°$) and still produce as-good a fit to the overall shock, as was reported by Hill et al in their virgin-lot study [4]. Effective boundary angles must be used by DSD to give optimum reproducibility of the complete set of wave-shape data; empirical boundary angles are typically adequate for this task. Fixed DSD boundary angles are used for all three PBX9502 $D(K)$ relations; 58° for unconfined HE, 62° for tin confinement and 65° for steel. The angles for tin and steel confinements take into account the thin layer of

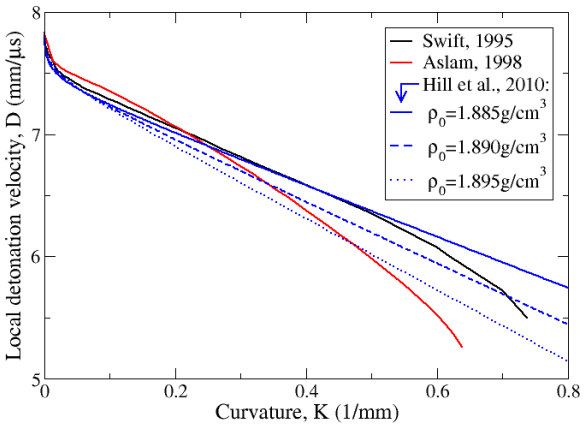

Figure 3. Detonation-velocity curvature relations for PBX9502.

gel between the two materials. A thin layer effectively decreases the confinement between two materials. The angles are estimated from simulations of steady-state detonation in a cylinder test where the detonation behaviour is controlled by the CREST reactive burn model [6].

The DSD model is used to calculate detonation burn-time isochrones in both 2D and 3D. The 2D model assumes there is an infinite charge depth and the component of detonation wave curvature is zero along the depth axis. The 3D model uses the finite depth of 10 cm and appropriate boundary constraints are imposed at the two ends of the cylinder. Due to the finite depth, the overall wave curvature should increase slightly which then would slow down the detonation wave compared to the 2D model. The timing of the DSD detonation is normalised to match the first experimental isochrone by way of minimising the sum of squared time residuals.

In the experiment, the proton radiography diagnostics were aimed down the depth of the cylinder. For each time snapshot, the full 3D detonation wave was captured on a single 2D image. Each image therefore represents an average density through the entire depth of the charge. However, since wavefront curvature is mainly confined to the edge, the radiograph roughly represents the tangent to the detonation wave at the centre line. Given this experimental error, DSD burn-time validation should take into account this uncertainty in timing. The DSD model sensitivity will be tested given the different $D(K)$ relations and dimensionality.

2.2. Validation metric

For quantitative comparison of DSD calculations to one another and also to past analysis, we describe the cross-section of the PBX9502 region in the same way as Terrones et al [1]. The distance from the origin is given by the polar function

$$h = \frac{(a+s)(b+cs)}{\sqrt{(a+s)^2\sin^2(\theta-30)+(b+cs)^2\cos^2(\theta-30)}}, \tag{1}$$

with parameters $a=4$, $b=3.3359$ and $c=1.6641$. The function when $s=0$ represents an inclined ellipse with major and minor axes a and b, i.e. charge inner surface, and when $s=1$ represents a circle of radius 5 cm, i.e. charge outer surface. The metric function is given by

$$\Delta T\left(t_{expt}, s\right) = t_{sim}\left(\theta_{expt}, s\right) - t_{expt}, \tag{2}$$

which serves as a quantitative measure of how well the DSD detonation wave is timed against experiment. A negative value of ΔT means that the calculated shock arrives sooner than that indicated by the experimental data. The overall error in detonation timing is encompassed in a global average metric, $\langle\Delta T\rangle = \frac{1}{N}\sum|\Delta T|$, for both upper and lower regions of the charge, denoted $\langle\Delta T\rangle_U$ and $\langle\Delta T\rangle_L$ respectively.

3. Results and discussion

For all PBX9502 $D(K)$ relations shown in figure 3, the global average metric is computed from 2D DSD calculations. The metric values are shown in table 1 and are comparable to those from previous DSD calculations by Terrones et al [1] where there was an average difference of ~ 60 ns.

Metric plots are shown for two isochrones for quantatitive comparison in figure 4. The density variation from Hill's $D(K)$ relation produces little change in detonation wave timing in the IHE experiment. However, the detonation wave propagation is too slow in the upper region, despite the fact that the $D(K)$ is calibrated to virgin material. The extra constraints placed on the $D(K)$ for additional temperatures and densities may have compromised its accuracy in the region of interest. The density effect is seen to be second order compared to the choice of $D(K)$ relation. Aslam's relation produces detonation propagation that evolves faster than experiment.

The wave-shape data used in Swift's calibration have curvatures no greater than 0.44mm^{-1}. The failure curvature of 0.74mm^{-1} in the $D(K)$ relation is a result of the form of non-linear function used in the $D(K)$ fitting process. Curvatures up to and including this failure value are experienced in the DSD calculations in regions of corner-turning (adjacent to the corners of the booster) and on the far inner surface of the charge. Similarly, curvatures smaller than the calibrated data are experienced where the detonation waves converge at the point furthest from the booster. This degree of extrapolation may lead to slight timing errors in the small regions affected. Since the same rate-stick diameter range was used for all three $D(K)$ calibrations, the amount of curvature extrapolation will be comparable for all of the DSD calculations.

Swift's relation produces the best overall 2D DSD result compared to the data, a more-complete set of results from which are shown in figures 5 and 6. The main discrepancy between DSD and experiment is for the lower region; the DSD timing is advanced compared to experiment, which is most apparent at times greater than $14\,\mu$s. This may be attributed to the occurance of a dead zone in the experiment around the corner of the PBX9501 booster which would delay the overall detonation wave, which is not accounted for in the simulation. The dead zone is thought to be larger for the lower region due to the effective detonation point being situated 2 mm below the centre-line of the booster. This would produce a sharper corner for the detonation wave to turn around and an overall delay in the lower region.

Table 1. Global average metric from 2D DSD calculations.

$D(K)$ for PBX9502	$\langle \Delta T \rangle_U$ (ns)	$\langle \Delta T \rangle_L$ (ns)	Overall match
Swift	59	65	Balanced
Aslam	45	93	Too fast
Hill (ρ_0 low→high)	89 / 92 / 96	51 / 47 / 48	All too slow

To test the 3D-ness of the IHE experiment, Swift's $D(K)$ relation was used in both 2D and 3D DSD calculations. Isochrones are shown in figure 7 to compare results from 2D, and 3D both on the mid-plane and the edge of the cylinder. It is found that, for the final isochrone, by going from 2D to 3D induces an average delay of ~ 40 ns at the mid-plane, which is significant enough to warrant a 3D code in order to correctly model the experiment and reproduce detonation wave timing to high precision. The move in 3D from the mid-plane to the edge induces a further delay of 110 ns, demonstrating the effect of varying detonation wave curvature along the depth of the charge and its significance in terms of detonation wave timing.

As seen from DSD calculations in 2D, Aslam's relation produced consistently fast results compared to experiment. To some extent this is compensated for by the delay brought in by

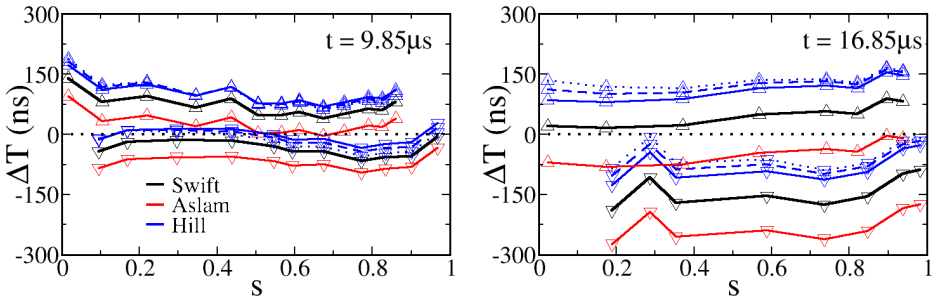

Figure 4. Metric plots from 2D DSD calculations for a range of PBX9502 $D(K)$ relations. Upwards triangles refer to the upper region and downwards triangles to the lower region. The legend for $D(K)$ relations is consistent with figure 3.

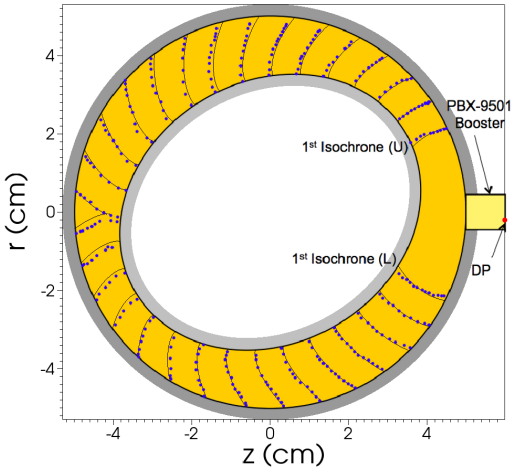

Figure 5. Detonation isochrones from 2D DSD calculation using Swift's $D(K)$ relation (solid lines) compared to experimental data (points) for isochrones at 3.85 to 17.85 μs in 1 μs intervals.

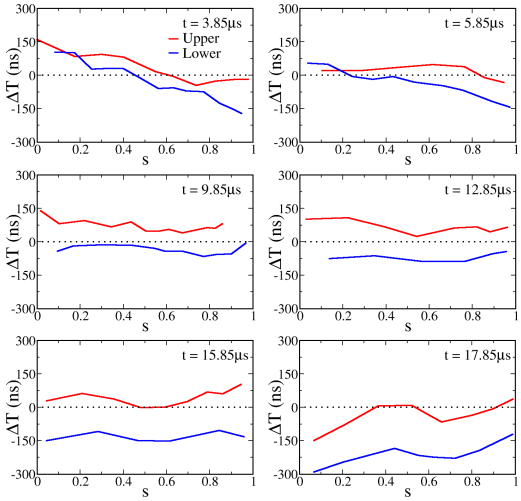

Figure 6. Metric plots from 2D DSD calculation using Swift's $D(K)$ relation for the upper (red) and lower (blue) halves of the IHE region.

going from 2D to 3D; metric plots are compared to the equivalent result using Swift's relation for a selection of isochrone times in figure 8. With this additional 3D delay, Swift's relation produces detonation isochrones that are too slow below 10 μs. Aslam's relation in 3D produces a better match to the data for the majority of isochrones both upper and lower regions. The exception still remains, however, for isochrones above 14 μs in the lower region; here the DSD detonation wave travels too quickly for reasons previously discussed.

4. Conclusions

The DSD model has been used to model the IHE experiment in both 2D and 3D. The delay in the detonation wave is on average $\sim$40 ns in by going from 2D to 3D (mid-plane) and a further 110 ns upon moving from the mid-plane to the charge edge. Of the three $D(K)$ relations tried, Swift's appears to give the best balanced results. The presence of dead zones (possibly larger in the lower segment) may have influenced the wave-shape in the experiment.

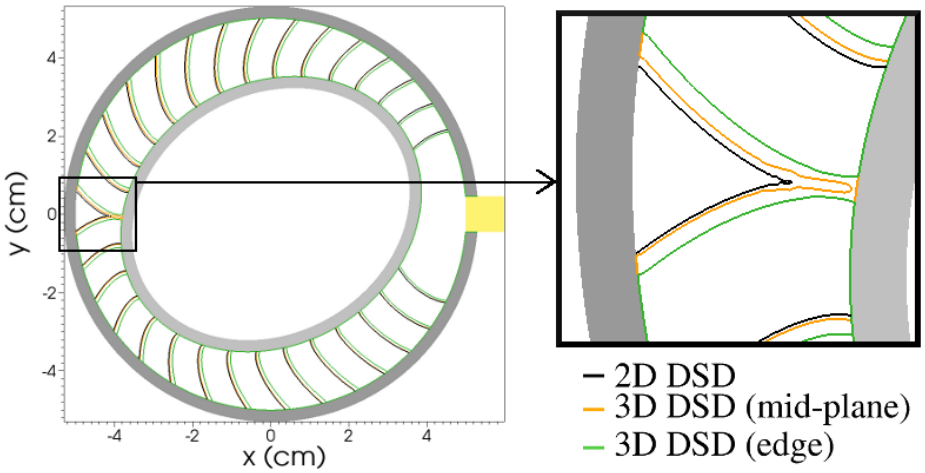

Figure 7. Detonation isochrones from 2D and 3D DSD calculations using Swift's $D(K)$ relation.

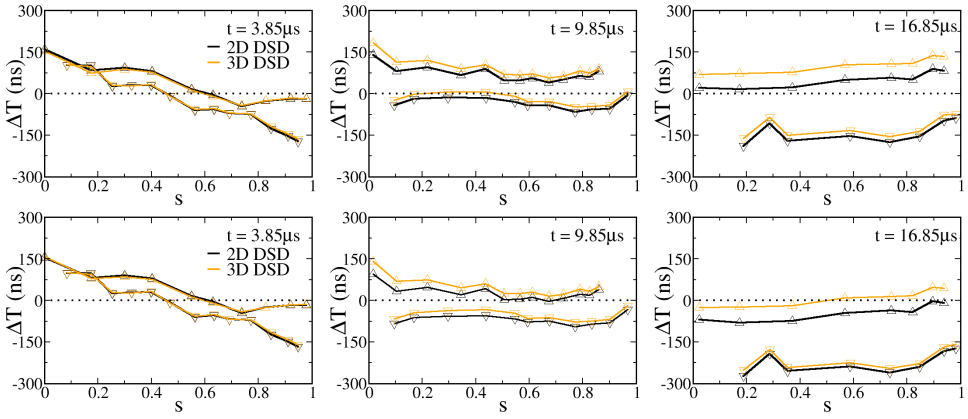

Figure 8. Metric plots from 2D (black) and 3D (orange) DSD calculations using Swift's (top 3 plots) and Aslam's (bottom 3 plots) $D(K)$ relations.

Acknowledgments

Thanks are due to Terrones et al and Los Alamos National Laboratory for kindly supplying and granting permission to re-publish their experimental data, Lawrence Livermore National Laboratory for supplying the PMESH code, and AWE staff supporting DSD development.

References

[1] Terrones G, Burkett M W and Morris C 2011 *AIP Conf. Proc.* **1426** 239
[2] Aslam T D 2007 *AIP Conf. Proc.* **955** 813
[3] Aslam T D, Bdzil J B and Hill L G 1998 *Proc. 11th Int. Det. Sym.* 21
[4] Hill L G and Aslam T D 2010 *Proc. 14th Int. Det. Sym.* 779
[5] Swift D C 1995 *Private Communication*
[6] Handley C A 2006 *Proc. 13th Int. Det. Sym.* 864